(Figure 6C) and the protein level (Figure 6D) by the same treatment. These results suggest that L-Glu was responsible for the decrease in L-Glu uptake during inflammation without cell death. When the microglia cultures were treated with LPS (10 ng/mL, 24 h) in the absence or presence of the hemichannel inhibitor, CBX (10 to 100 μM), the L-Glu release from the activated microglia was suppressed in a concentration-dependent manner (Figure 7A). CBX (100 μM) almost completely prevented the LPS-induced (10 ng/mL, 72 h) decrease in L-Glu uptake in the mixed culture (Figure 7B, left) but had no effect in the astrocyte culture (Figure 7B, right). Furthermore, CBX reversed the LPS-induced downregulation of GLAST expression at the mRNA (Figure 7C) and protein levels (Figure 7D).

We next tried to clarify the mechanisms through which the sustained elevation of extracellular L-Glu downregulates GLAST. Recent reports have suggested that the expression of L-Glu transporters is regulated by L-Glu through metabotropic glutamate receptors (mGluRs). We therefore first examined the involvement of metabotropic glutamate receptors (mGluRs). Neither the group I mGluR agonist DHPG nor the group II mGluR agonist DCG-4 affected either L-Glu uptake

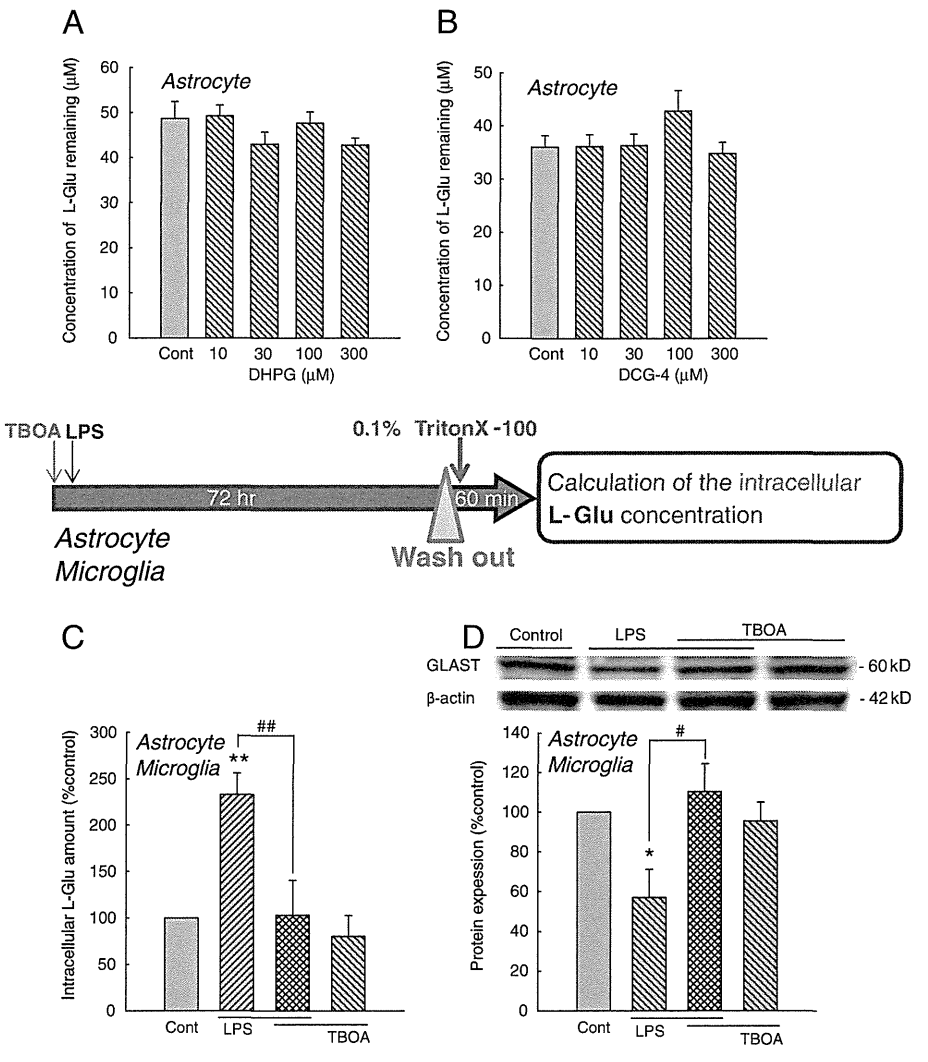

Figure 8 The elevation of intracellular L-Glu in astrocytes is important for the downregulation of GLAST. (**A**, **B**) The effects of mGluR agonists on L-Glu uptake. Neither the group I mGluR agonist DHPG (A) nor the group II mGluR agonist DCG-4 (B) affected L-Glu uptake. (**C**) The amount of astrocytic intracellular L-Glu after LPS-treatment in the absence or presence of TBOA in astrocyte-microglia co-cultures. LPS significantly increased the amount of astrocytic intracellular L-Glu, and TBOA completely suppressed this increase. $^{**}P < 0.01$ *vs.* control group, $^{\#\#}P < 0.01$ *vs.* the LPS-treated group ($n = 6$), Tukey's test following ANOVA. (**D**) The astrocytic expression of GLAST after LPS treatment in the absence or presence of TBOA in astrocyte-microglia co-cultures. TBOA suppressed the downregulation GLAST caused by LPS. $^{*}P < 0.05$ *vs.* control group, $^{\#}P < 0.05$ *vs.* the LPS-treated group ($n = 6$), Tukey's test following ANOVA.

(Figure 8A and B) or the expression level of GLAST (not shown). Sustained elevation of extracellular L-Glu caused by activated microglia is expected to cause the elevation of intracellular L-Glu in astrocytes. We therefore examined whether the elevation of intracellular L-Glu itself is important for the downregulation of GLAST. To do this, we first measured the amount of astrocytic intracellular L-Glu after LPS-treatment in the absence or presence of TBOA in astrocyte-microglia co-cultures (Figure 8C). LPS significantly increased the amount of intracellular L-Glu, and TBOA completely suppressed this increase. Western blotting showed that TBOA suppressed the downregulation GLAST caused by LPS (Figure 8D). TBOA itself did not have effects on either the amount of intracellular L-Glu or the GLAST protein level. These results indicate that the elevation of astrocytic intracellular L-Glu, but not the signaling cascade from the cell surface, is important for the downregulation of GLAST.

Our findings suggest that activated microglia trigger the elevation of extracellular L-Glu through their own release of L-Glu, astrocyte L-Glu transporters are downregulated by the elevation of astrocytic intracellular L-Glu, and further elevation of extracellular L-Glu occurs early in neuroinflammation. A schematic model of this 'collusion' hypothesis is shown in Figure 9.

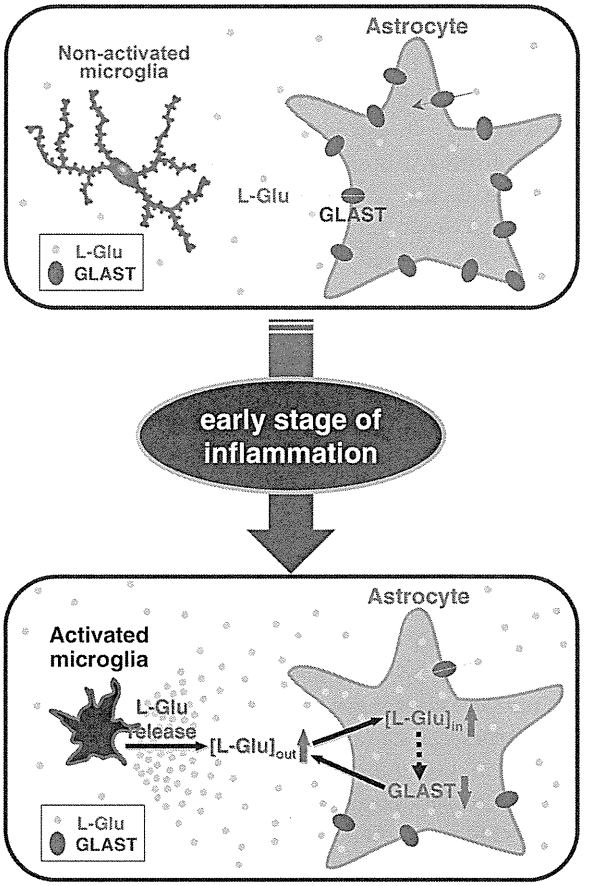

Figure 9 Schematic model of the 'collusion' hypothesis for the elevation of extracellular L-Glu in the early stages of inflammation. 1. Activated microglia release L-Glu. 2. The resultant elevation of extracellular L-Glu causes the elevation of astrocytic intracellular L-Glu. 3. The elevation of astrocytic intracellular L-Glu downregulates GLAST expression. 4. The decrease in GLAST expression further exacerbates the elevation of extracellular L-Glu.

Discussion

To quantify L-Glu transporter function, we measured the extracellular concentrations of L-Glu 30 min after a single exogenous application of L-Glu to the medium (the starting concentration was 100 μM). To limit any contributions of extra L-Glu from dying cells, and to verify a substantial contribution of the decrease in L-Glu transport potency to an elevated concentration of extracellular L-Glu in inflammation, we first determined the optimal conditions for inflammation without cell death. We used a lower concentration of LPS (10 ng/mL) than is generally used [35,36]. LPS application at a concentration of 10 ng/mL for 72 h activated the microglia but did not cause either LDH leakage or decreases in MTT reduction in the mixed culture, astrocyte pure culture, or microglia pure culture. LPS induces an inflammatory response in microglia via Toll-like receptor 4 (TLR4) [37]. TLR4 is also expressed by astrocytes, and astrocytes themselves have shown inflammatory responses in response to LPS in some reports [38]. In the present study, however, microglia were essential for the decreased L-Glu by astrocytes, and LPS did not affect L-Glu uptake in astrocyte cultures. Because the expression of TLR4 by astrocytes is less than that of microglia [37], the LPS stimulation in our model of inflammation without cell death may be insufficient to induce phenotypic changes in astrocytes. These mild inflammatory conditions may reflect the early stages of neuroinflammation *in vivo*, in which early microglial activation has been observed to precede the phenotypic changes in astrocytes [39].

In the present study, we pharmacologically confirmed that GLAST, and not GLT-1, was the predominant functional L-Glu transporter. We also confirmed that the expression level of GLT-1 is much lower than that of GLAST. GLT-1 has been reported to be functional in neuron-astrocyte co-cultures at 32 to 44 DIV [40]. This discrepancy most likely arises from the maturation stages of neurons, as the functional development of GLT-1 correlates with neuronal maturation [41]. The expression of GLAST was significantly decreased in the 'non-cell death inflammation model', which indicates that the decrease in L-Glu uptake in this inflammation model was mainly caused by the downregulation of GLAST.

Activated microglia release various soluble factors, including inflammatory cytokines [18,19], reactive oxygen species [20], NO [16], L-Glu [21,22], and ATP [23,24]. We demonstrated that L-Glu is the factor that downregulates GLAST in astrocytes during inflammation without cell death. Although activated microglia are known to release L-Glu through hemichannels [21,22], the neurological importance of this phenomenon remains unclear. We showed that the hemichannel inhibitor CBX completely suppressed the release of L-Glu from microglia, the decrease in L-Glu uptake, and the downregulation of GLAST expression during inflammation without cell death. These data provide strong evidence that L-Glu is the microglial releasing factor that downregulates GLAST. High concentrations of ATP have also been shown to downregulate GLAST through the P2X7 receptor [28]. However, we believe that ATP did not contribute to the down-regulation of GLAST in the inflammation model without cell death here because L-Glu uptake did not change when the astrocyte culture was treated with ATP (Figure 5A) or the P2X7 agonist BzATP (Figure 5B). We also confirmed that neither the P2X receptor antagonist TNP-ATP (Figure 5C) nor the P2X7-specific antagonist BBG (Figure 5D) inhibited the decrease in L-Glu uptake in this inflammation model. Other microglial releasing factors, such as TNF-α, IL-1β, and arachidonic acid, are also known to decrease the L-Glu transport in astrocyte cultures [25-27]. However, the conditioned media collected from our model of inflammation without cell death had no effect in the astrocyte culture. Because the LPS stimulation here was lower than that of other studies [35,36] (to prevent cell death), the amount of these factors in the conditioned media may have been insufficient to affect L-Glu transporters.

Recent reports have suggested that the expression of L-Glu transporters is regulated by L-Glu through metabotropic glutamate receptors (mGluRs), that is, the group I mGluR agonist downregulates GLAST, whereas the group II mGluR agonist has the opposite effect [42,43]. However, neither the group I mGluR agonist nor the group II mGluR agonist affected the expression of GLAST in the present study. Instead, we clarified that the elevation of intracellular L-Glu in astrocytes is important for the downregulation of GLAST as shown in Figure 8. It has been clarified that translation initiation is regulated by intracellular L-Glu transported by GLAST in Bergmann glial cells [44,45]. They also showed that mammalian target of rapamycin (mTOR), increase in intracellular Ca^{2+} levels, and p60(Src)/PI3K/PKB pathway are involved in this regulation. Further investigation is necessary to confirm whether the same pathways are involved in the downregulation of GLAST observed in our study. Of interest, a sustained elevation of extracellular L-Glu induced by the same protocol as Figure 6 did not cause the downregulation of glutamine synthetase (GS) in our preliminary experiment (data not shown), suggesting that this regulation is GLAST or L-Glu transporter-specific. The comparison of the upstream DNA sequences of GLAST and GS might provide useful information. Besides, in *Saccharomyces cerevisiae*, the activator (NIL1p) of the amino acid transporter is inactivated by increases in intracellular glutamate [46]. It is possible that a conserved mechanism similar to this also exist in astrocytes. Our findings strongly suggest that L-Glu is the microglial releasing factor which results in downregulation of GLAST in the early stage of inflammation. However, whether or not the quantity of L-Glu released from microglia is enough to induce a range of reaction still needs to be elucidated. Based on the discussion above, the co-factors to enhance the signaling pathway in the astrocytes leading to the downregulation of GLAST might be also released from microglia.

Conclusions

Our findings suggest that activated microglia trigger the elevation of extracellular L-Glu through their own release of L-Glu, astrocyte L-Glu transporters are downregulated by the elevation of astrocytic intracellular L-Glu, and further elevation of extracellular L-Glu is caused as an early event of neuroinflammation (Figure 9).

Abbreviations

ANOVA: Analysis of variance; ATP: Adenosine 5′-triphosphate disodium salt hydrate; BPB: Bromophenol blue sodium salt; BSA: Albumin bovine serum; BzATP: 2′ (3′)-O-(4-Benzoylbenzoyl)ATP triethylammonium salt; CBX: Carbenoxolone; CNS: Central nervous system; DHK: Dihydrokainic acid; DIV: Days *in vitro*; DMEM: Dulbecco's modified eagle medium; DNA: Deoxyribonucleic acid; EDTA: Ethylenediaminetetraacetate; EGTA: Ethyleneglycoldiaminetetraacetate; FBS: Fetal bovine serum; GFAP: Glial fibrillary acidic protein; GlDH: Glutamate dehydrogenase; HS: Horse serum; LDH: Lactate dehydrogenase; L-Glu: L-glutamate; LPS: Lipopolysaccharide; mGluRs: Metabotropic glutamate receptors; MPMS: 1-methoxy-5-methylphenazinium methyl sulfate; MTT: 3-(4,5-dimethyl-2-thiazolyl)-2,5-diphenyl-2H-tetrazolium bromide; β-NAD: β-nicotinamide adenine dinucleotide; NO: Nitric oxide; NP-40: Polyoxyethylene(9)octylphenyl ether; OxATP: Adenosine 5′-triphosphate periodate oxidized sodium salt; PBS: Phosphate-buffered saline; PFA: Paraformaldehyde; RNA: Ribonucleic acid; RT-PCR: Polymerase chain reaction; SD: Sprague–Dawley; SDS: Sodium dodecyl sulfate; TBOA: DL-threo-β-benzyloxyaspartic acid; TLR4: Toll-like receptor 4; TNP-ATP: 2′,3′-O-(2,4,6-Trinitrophenyl)ATP salt hydrate; Tris–HCl: Tris (hydroxymethyl) aminomethane; Tuj1: β3 tubulin; UCPH 101: 2-Amino-5,6,7,8-tetrahydro-4-(4-methoxyphenyl)-7-(naphthalen-1-yl)-5-oxo-4H-chromene-3-carbonitrile.

Competing interests

I declare that I have no significant competing financial, professional or personal interests that might have influenced the performance or presentation of the work described in this manuscript.

Authors' contributions

JT performed experimental work and manuscript writing. KF performed experimental work. MM performed additional experimental work. TS provided advice on the experimental direction. YS provided advice on manuscript writing and preparation. KS designed the biological experimental plan and performed biological experiments, data analysis, manuscript writing, and preparation. All authors have read and approved the final version of the manuscript.

Acknowledgements
This study was partly supported by a Grant-in-Aid from the Food Safety Commission of Japan (No. 1003); a Grant-in-Aid for Young Scientists from MEXT, Japan (KAKENHI 21700422); the Program for the Promotion of Fundamental Studies in Health Sciences of NIBIO, Japan; a Health and Labor Science Research Grant for Research on Risks of Chemicals; and a Health and Labor Science Research Grant for Research on New Drug Development from MHLW, Japan, awarded to KS and YS.

Author details
[1]Laboratory of Neuropharmacology, Division of Pharmacology, National Institute of Health Sciences, 1-18-1 Kamiyoga, Setagaya-ku, Tokyo 158-8501, Japan. [2]Division of Basic Biological Science, Faculty of Pharmacy, Keio University, 1-5-30 Shiba-koen, Minato-ku, Tokyo 105-8512, Japan.

Received: 25 May 2012 Accepted: 1 December 2012
Published: 23 December 2012

References

1. Kumar A, Singh RL, Babu GN: **Cell death mechanisms in the early stages of acute glutamate neurotoxicity.** *Neurosci Res* 2010, **66**:271–278.
2. Choi DW: **Glutamate neurotoxicity and diseases of the nervous system.** *Neuron* 1988, **1**:623–634.
3. Rothstein JD, Dykes-Hoberg M, Pardo CA, Bristol LA, Jin L, Kuncl RW, Kanai Y, Hediger MA, Wang Y, Schielke JP, Welty DF: **Knockout of glutamate transporters reveals a major role for astroglial transport in excitotoxicity and clearance of glutamate.** *Neuron* 1996, **16**:675–686.
4. Lauderback CM, Harris-White ME, Wang Y, Pedigo NW Jr, Carney JM, Butterfield DA: **Amyloid beta-peptide inhibits Na^+-dependent glutamate uptake.** *Life Sci* 1999, **65**:1977–1981.
5. Rothstein JD: **Excitotoxicity and neurodegeneration in amyotrophic lateral sclerosis.** *Clin Neurosci* 1995–1996, **3**:348–359.
6. Choudary PV, Molnar M, Evans SJ, Tomita H, Li JZ, Vawter MP, Myers RM, Bunney WE Jr, Akil H, Watson SJ, Jones EG: **Altered cortical glutamatergic and GABAergic signal transmission with glial involvement in depression.** *Proc Natl Acad Sci USA* 2005, **102**:15653–15658.
7. Beart PM, O'Shea RD: **Transporters for L-glutamate: an update on their molecular pharmacology and pathological involvement.** *Br J Pharmacol* 2007, **150**:5–17.
8. Guo F, Sun F, Yu JL, Wang QH, Tu DY, Mao XY, Liu R, Wu KC, Xie N, Hao LY, Cai JQ: **Abnormal expressions of glutamate transporters and metabotropic glutamate receptor 1 in the spontaneously epileptic rat hippocampus.** *Brain Res Bull* 2010, **81**:510–516.
9. Rakhade SN, Loeb JA: **Focal reduction of neuronal glutamate transporters in human neocortical epilepsy.** *Epilepsia* 2008, **49**:226–236.
10. Proper EA, Hoogland G, Kappen SM, Jansen GH, Rensen MG, Schrama LH, van Veelen CW, van Rijen PC, van Nieuwenhuizen O, Gispen WH, de Graan PND: **Distribution of glutamate transporters in the hippocampus of patients with pharmaco-resistant temporal lobe epilepsy.** *Brain* 2002, **125**:32–43.
11. Ward RJ, Colivicchi MA, Allen R, Schol F, Lallemand F, de Witte P, Ballini C, Corte LD, Dexter D: **Neuro-inflammation induced in the hippocampus of 'binge drinking' rats may be mediated by elevated extracellular glutamate content.** *J Neurochem* 2009, **111**:1119–1128.
12. Castillo J, Dávalos A, Alvarez-Sabín J, Pumar JM, Leira R, Silva Y, Montaner J, Kase CS: **Molecular signatures of brain injury after intracerebral hemorrhage.** *Neurology* 2002, **58**:624–629.
13. Allen NJ, Barres BA: **Neuroscience: Glia - more than just brain glue.** *Nature* 2009, **457**:675–677.
14. Lehnardt S: **Innate immunity and neuroinflammation in the CNS: the role of microglia in Toll-like receptor-mediated neuronal injury.** *Glia* 2010, **58**:253–263.
15. Perry VH, Nicoll JA, Holmes C: **Microglia in neurodegenerative disease.** *Nat Rev Neurol* 2010, **6**:193–201.
16. Kreutzberg GW: **Microglia: a sensor for pathological events in the CNS.** *Trends Neurosci* 1996, **19**:312–318.
17. Lynch MA: **The multifaceted profile of activated microglia.** *Mol Neurobiol* 2009, **40**:139–156.
18. Hanisch UK: **Microglia as a source and target of cytokines.** *Glia* 2002, **40**:140–155.
19. Nakajima K, Kohsaka S: **Microglia: activation and their significance in the central nervous system.** *J Biochem* 2001, **130**:169–175.
20. Block ML, Hong JS: **Chronic microglial activation and progressive dopaminergic neurotoxicity.** *Biochem Soc Trans* 2007, **35**:1127–1132.
21. Takeuchi H, Jin S, Wang J, Zhang G, Kawanokuchi J, Kuno R, Sonobe Y, Mizuno T, Suzumura A: **Tumor necrosis factor-alpha induces neurotoxicity via glutamate release from hemichannels of activated microglia in an autocrine manner.** *J Biol Chem* 2006, **281**:21362–21368.
22. Yawata I, Takeuchi H, Doi Y, Liang J, Mizuno T, Suzumura A: **Macrophage-induced neurotoxicity is mediated by glutamate and attenuated by glutaminase inhibitors and gap junction inhibitors.** *Life Sci* 2008, **82**:1111–1116.
23. Higashi Y, Segawa S, Matsuo T, Nakamura S, Kikkawa Y, Nishida K, Nagasawa K: **Microglial zinc uptake via zinc transporters induces ATP release and the activation of microglia.** *Glia* 2011, **59**:1933–1945.
24. Kim SY, Moon JH, Lee HG, Kim SU, Lee YB: **ATP released from beta-amyloid-stimulated microglia induces reactive oxygen species production in an autocrine fashion.** *Exp Mol Med* 2007, **39**:820–827.
25. Carmen J, Rothstein JD, Kerr DA: **Tumor necrosis factor-alpha modulates glutamate transport in the CNS and is a critical determinant of outcome from viral encephalomyelitis.** *Brain Res* 2009, **1263**:143–154.
26. Prow NA, Irani DN: **The inflammatory cytokine, interleukin-1 beta, mediates loss of astroglial glutamate transport and drives excitotoxic motor neuron injury in the spinal cord during acute viral encephalomyelitis.** *J Neurochem* 2008, **105**:1276–1286.
27. Volterra A, Trotti D, Racagni G: **Glutamate uptake is inhibited by arachidonic acid and oxygen radicals via two distinct and additive mechanisms.** *Mol Pharmacol* 1994, **46**:986–992.
28. Liu YP, Yang CS, Chen MC, Sun SH, Tzeng SF: **Ca(2+)-dependent reduction of glutamate aspartate transporter GLAST expression in astrocytes by P2X(7) receptor-mediated phosphoinositide 3-kinase signaling.** *J Neurochem* 2010, **113**:213–227.
29. Sato K, Matsuki N, Ohno Y, Nakazawa K: **Estrogens inhibit l-glutamate uptake activity of astrocytes via membrane estrogen receptor alpha.** *J Neurochem* 2003, **86**:1498–1505.
30. Sato K, Saito Y, Oka J, Ohwada T, Nakazawa K: **Effects of tamoxifen on L-glutamate transporters of astrocytes.** *J Pharmacol Sci* 2008, **107**:226–230.
31. Nakajima K, Shimojo M, Hamanoue M, Ishiura S, Sugita H, Kohsaka S: **Identification of elastase as a secretory protease from cultured rat microglia.** *J Neurochem* 1992, **58**:1401–1408.
32. Kohl A, Dehghani F, Korf HW, Hailer NP: **The bisphosphonate clodronate depletes microglial cells in excitotoxically injured organotypic hippocampal slice cultures.** *Exp Neurol* 2003, **181**:1–11.
33. Abe K, Matsuki N: **Measurement of cellular 3-(4,5-dimethylthiazol-2-yl)-2,5-diphenyltetrazolium bromide (MTT) reduction activity and lactate dehydrogenase release using MTT.** *Neurosci Res* 2000, **38**:325–329.
34. Wink MR, Braganhol E, Tamajusuku AS, Lenz G, Zerbini LF, Libermann TA, Sévigny J, Battastini AM, Robson SC: **Nucleoside triphosphate diphosphohydrolase-2 (NTPDase2/CD39L1) is the dominant ectonucleotidase expressed by rat astrocytes.** *Neuroscience* 2006, **138**:421–432.
35. Li J, Ramenaden ER, Peng J, Koito H, Volpe JJ, Rosenberg PA: **Tumor necrosis factor alpha mediates lipopolysaccharide-induced microglial toxicity to developing oligodendrocytes when astrocytes are present.** *J Neurosci* 2008, **28**:5321–5330.
36. Bal-Price A, Brown GC: **Inflammatory neurodegeneration mediated by nitric oxide from activated glia-inhibiting neuronal respiration, causing glutamate release and excitotoxicity.** *J Neurosci* 2001, **21**:6480–6491.
37. Lehnardt S, Lachance C, Patrizi S, Lefebvre S, Follett PL, Jensen FE, Rosenberg PA, Volpe JJ, Vartanian T: **The toll-like receptor TLR4 is necessary for lipopolysaccharide-induced oligodendrocyte injury in the CNS.** *J Neurosci* 2002, **22**:2478–2486.
38. Carpentier PA, Begolka WS, Olson JK, Elhofy A, Karpus WJ, Miller SD: **Differential activation of astrocytes by innate and adaptive immune stimuli.** *Glia* 2005, **49**:360–374.
39. Tilleux S, Hermans E: **Neuroinflammation and regulation of glial glutamate uptake in neurological disorders.** *J Neurosci Res* 2007, **85**:2059–2070.
40. Swanson RA, Liu J, Miller JW, Rothstein JD, Farrell K, Stein BA: **Longuemare MC: Neuronal regulation of glutamate transporter subtype expression in astrocytes.** *J Neurosci* 1997, **17**:932–940.

41. Perego C, Vanoni C, Bossi M, Massari S, Basudev H, Longhi R, Pietrini G: **The GLT1 and GLAST glutamate transporters are expressed on morphologically distinct astrocytes and regulated by neuronal activity in primary hippocampal cocultures.** *J Neurochem* 2000, **75**:1076–1084.
42. Gegelashvili G, Dehnes Y, Danbolt NC, Schousboe A: **The high-affinity glutamate transporters GLT1, GLAST, and EAAT4 are regulated via different signalling mechanisms.** *Neurochem Int* 2000, **37**:163–170.
43. Aronica E, Gorter JA, Ijlst-Keizers H, Rozemuller AJ, Yankaya B, Leenstra S, Troost D: **Expression and functional role of mGluR3 and mGluR5 in human astrocytes and glioma cells: opposite regulation of glutamate transporter proteins.** *Eur J Neurosci* 2003, **17**:2106–2118.
44. González-Mejia ME, Morales M, Hernández-Kelly LC, Zepeda RC, Bernabé A, Ortega A: **Glutamate-dependent translational regulation in cultured Bergmann glia cells: involvement of p70S6K.** *Neuroscience* 2006, **141**:1389–1398.
45. Zepeda RC, Barrera I, Castelán F, Suárez-Pozos E, Melgarejo Y, González-Mejia E, Hernández-Kelly LC, López-Bayghen E, Aguilera J, Ortega A: **Glutamate-dependent phosphorylation of the mammalian target of rapamycin (mTOR) in Bergmann glial cells.** *Neurochem Int* 2009, **55**:282–287.
46. Stanbrough M, Rowen DW, Magasanik B: **Role of the GATA factors Gln3p and Nil1p of Saccharomyces cerevisiae in the expression of nitrogen-regulated genes.** *Proc Natl Acad Sci USA* 1995, **92**:9450–9454.

doi:10.1186/1742-2094-9-275
Cite this article as: Takaki *et al.*: L-glutamate released from activated microglia downregulates astrocytic L-glutamate transporter expression in neuroinflammation: the 'collusion' hypothesis for increased extracellular L-glutamate concentration in neuroinflammation. *Journal of Neuroinflammation* 2012 **9**:275.

ACS Chemical Neuroscience

Research Article

pubs.acs.org/acschemicalneuroscience

Discovery of a Tamoxifen-Related Compound that Suppresses Glial L-Glutamate Transport Activity without Interaction with Estrogen Receptors

Kaoru Sato,*[,‡,†] Jun-ichi Kuriwaki,[‡,†] Kanako Takahashi,[‡] Yoshihiko Saito,[§] Jun-ichiro Oka,[§] Yuko Otani,[∥] Yu Sha,[∥] Ken Nakazawa,[‡] Yuko Sekino,[‡] and Tomohiko Ohwada*[,∥]

[‡]Laboratory of Neuropharmacology, Division of Pharmacology, National Institute of Health Sciences, 1-18-1 Kamiyoga, Setagaya-ku, Tokyo 158-8501, Japan

[§]Laboratory of Pharmacology, Faculty of Pharmaceutical Sciences, Tokyo University of Science, 2541 Yamazaki, Noda-city, Chiba 278-8510, Japan

[∥]Laboratory of Organic and Medicinal Chemistry, Graduate School of Pharmaceutical Sciences, University of Tokyo, 7-3-1, Hongo, Bunkyo-ku, Tokyo 113-0033, Japan

ABSTRACT: We recently found that tamoxifen suppresses L-glutamate transport activity of cultured astrocytes. Here, in an attempt to separate the L-glutamate transporter-inhibitory activity from the estrogen receptor-mediated genomic effects, we synthesized several compounds structurally related to tamoxifen. Among them, we identified two compounds, **1** (YAK01) and **3** (YAK037), which potently inhibited L-glutamate transporter activity. The inhibitory effect of **1** was found to be mediated through estrogen receptors and the mitogen-activated protein kinase (MAPK)/phosphatidylinositol 3-kinase (PI3K) pathway, though **1** showed greatly reduced transactivation activity compared with that of 17β-estradiol. On the other hand, compound **3** exerted its inhibitory effect through an estrogen receptor-independent and MAPK-independent, but PI3K-dependent pathway, and showed no transactivation activity. Compound **3** may represent a new platform for developing novel L-glutamate transporter inhibitors with higher brain transfer rates and reduced adverse effects.

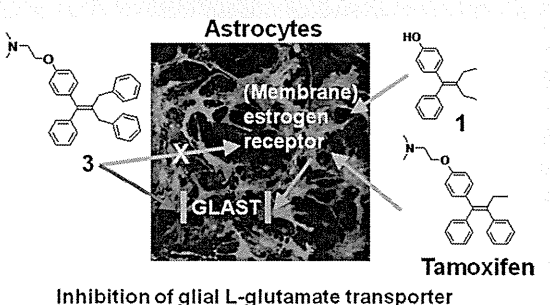

Inhibition of glial L-glutamate transporter

KEYWORDS: *Tamoxifen, astrocyte, L-glutamate transporter, ERα, tetrasubstituted ethylene, nongenomic pathway*

L-Glutamate (L-Glu) is one of the major excitatory neurotransmitters in the central nervous system (CNS), but high concentrations of extracellular L-Glu cause excessive stimulation of L-Glu receptors in the CNS, leading to neurotoxicity.[1,2] Astrocyte L-Glu transporters are the only machinery available to remove L-Glu from extracellular fluid and to maintain a low and nontoxic concentration of L-Glu.[3] Consequently, dysfunction of astrocyte L-Glu transporters is considered to be implicated in the pathology of neurodegenerative conditions.[4] Therefore, exogenous compounds that can regulate the function of L-Glu transporters may provide chemical tools to investigate the regulatory mechanisms of these transporters at the molecular level, and would also be candidate therapeutic agents.

There is growing evidence that estrogen receptor (ER) α, which is a nuclear ER (nER) that mediates genomic effects, can also be translocated to plasma membranes and mediate acute nongenomic effects in some cases. We have clarified that 17β-estradiol (E2) inhibits L-Glu transporters via a nongenomic pathway involving membrane-associated ERα (mERα).[5] Tamoxifen (Tam), a synthetic estrogen analogue that is clinically used in the treatment of breast cancer to block the proliferative action of estrogens,[6] also inhibited astrocyte L-Glu transporters at picomolar concentration, probably through the same nongenomic pathway as E2.[7] Because overexpression of astrocyte L-Glu transporters is often associated with neuropsychiatric disorders,[4] inhibitors of L-Glu transporters may be clinically useful to ameliorate these disorders.[8] However, Tam also acts on genomic pathways involving nuclear estrogen receptors (nERs) α and β, depending on the cell type and promoter context,[9] and so may cause adverse effects including endometrial changes, depression and weight gain.[10,11] Therefore, Tam-inspired compounds that retain the inhibitory effect on L-Glu transporters, but lack the nER-mediated genomic effects, would be useful tools for biological research, as well as candidate therapeutic agents.

Tam is a tetrasubstituted triphenylethylene derivative, in which the four substituents on the olefinic carbon atoms are different. This structural complexity makes the stereospecific synthesis of Tam-related derivatives difficult. We thus focused on Tam-inspired compounds bearing identical substituents on at least one of the olefinic carbon atoms.[12] It is well-known that the *N*,*N*-dimethylaminoethyl substituent on the phenolic oxygen atom and the regiochemistry of the tetrasubstituted

Received: September 29, 2011
Accepted: November 14, 2011
Published: November 14, 2011

olefin of Tam are crucial for ER binding activity.[13] So, we considered that more symmetrical derivatives of Tam might show reduced ER-binding ability.

Among our synthesized compounds, we found two, compounds **1** (YAK01) and **3** (YAK037), with potent L-Glu transporter-inhibitory activity. Studies of their mechanisms of action indicated that, unlike Tam, compound **3** acts through an ER-independent and MAPK-independent, but PI3K-dependent pathway and shows no transactivation activity for nERs. We believe this compound may represent a new platform for developing novel L-Glu transporter inhibitors with higher brain transfer rates and reduced adverse effects.

RESULTS AND DISCUSSION

We synthesized several Tam-inspired compounds bearing identical substituents on one carbon atom of the olefin,[12] and found that two of them were potent inhibitors of astrocyte L-Glu transporters. The diethyl-substituted derivative **1** inhibited L-Glu transporters in the picomolar range (62.7 ± 7.48% of control at 1 pM; Figure 2A). The dose–response curve for the inhibitory activity was not linear, but followed an inverted U-shaped curve; however, such a non-monotonic dose dependence is rather common for hormones and their mimetics.[14] On the other hand, when the symmetrical substituent was changed from ethyl to benzyl (**2**), the inhibitory effect was lost (Figure 2B). However, when the phenolic oxygen atom of **1** was substituted with a *N,N*-dimethylaminoethyl group (Figure 1C), we found

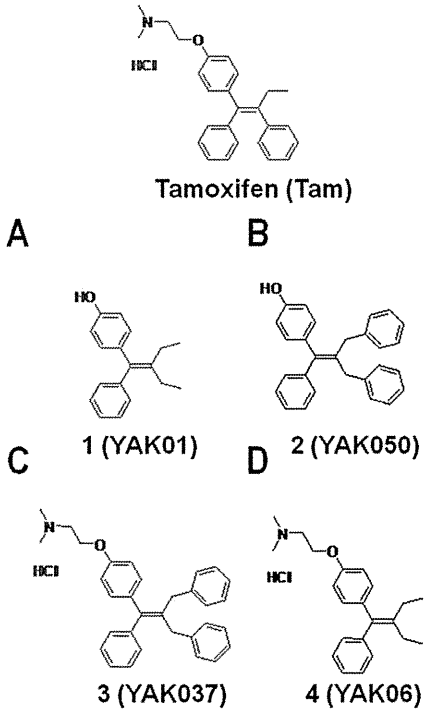

Figure 1. Chemical structures of the newly synthesized tamoxifen-related compounds.

that the resulting compound **3** showed dose-dependent L-Glu transporter inhibition in the picomolar range (63.8 ± 5.49% of control at 1 pM; Figure 2C). The dose-dependency of the effect of **3** suggested that the underlying mechanism might be different from that in the case of **1**. Compound **4** was inactive (Figure 2D).

We next examined the effects of **1** and **3** on cell viability by means of MTT reduction assay and LDH leakage assay, using the same cultured sample. Neither of the compounds was cytotoxic at concentrations below 1 μM (Figure 3), though 100 μM **1** and 10 μM **3** caused severe cell damage. These results exclude the possibility that the L-Glu clearance-inhibitory effects of these compounds at concentrations below 1 μM were caused by cell damage.

In order to confirm the involvement of L-Glu transporters in the inhibition of L-Glu uptake by our compounds, and to rule out the possibility that **1** and **3** act by inducing L-Glu release from astrocytes, we next examined the effect of **1** and **3** on L-Glu clearance when the L-Glu transporter activity was blocked with TBOA, a potent nonselective L-Glu transporter inhibitor (IC_{50}: 48 μM for GLAST/EAAT1, 7 μM for GLT1/EAAT2). We confirmed that application of 1 mM TBOA potently inhibited L-Glu transporter activity; that is, TBOA caused reversible chemical knock-down of L-Glu transporter activity.[7] When either **1** or **3** was coapplied with 1 mM TBOA, these compounds no longer influenced L-Glu clearance (Figure 4), indicating that the actions of these compounds are indeed mediated by L-Glu transporters, and do not involve L-Glu release from astrocytes.

Our cultured astrocytes predominantly expressed ERα, and little or no expression of ERβ was detected.[5] Tam is known to be a partial agonist of ERs,[9] raising the possibility that the compounds exerted their inhibitory effects via interaction with ERα. Therefore, we examined the involvement of ERα by coapplication of ICI182,780, a high-affinity antagonist of ERs. ICI182,780 dose-dependently blocked the inhibition of L-Glu uptake caused by **1** (Figure 5A) at 0.01, 0.1, and 1 μM, at which the effects of Tam were reported to be completely suppressed.[7] In contrast, ICI182,780 had no effect on the inhibition by **3** (Figure 5B), suggesting that the mechanism of the inhibition by **3** is independent of ERs. We further examined the signal transduction pathways mediating the effects of **1** and **3**. When coapplied with U0126, which inhibits mitogen-activated protein kinase/extracellular signal-regulated kinase 1 (MEK1, IC50: 70 nM) and MEK2 (IC50: 60 nM), the inhibitory effect by **1** was blocked, whereas that of **3** was not (Figure 6A). On the other hand, when coapplied with LY294002, a specific phosphoinositide 3-kinase (PI3K) inhibitor (IC50: 70 nM), the inhibitory effects of both compounds were completely blocked (Figure 6B). These results suggest that PI3K is a common mediator of the effects of both compounds, whereas mitogen-activated protein kinase (MAPK) is involved only in the mechanism of inhibition by **1**.

Finally we examined the ER-agonist potency of **1** and **3**, i.e., the transcriptional effects of these compounds via human ERα and ERβ, using HEK293/hERα and HEK293/hERβ reporter cells (Figure 7). Compound **1** showed agonist activity in both of 293/hERα and 293/hERβ reporter cells, though the binding affinities were much weaker than that of E2. The EC50 values of **1** for ERα and ERβ are 30.8 nM and 10.4 nM, respectively (1.25 nM and 0.864 nM, respectively, for E2). The relative agonist activity of **1** was 66.8% of that of E2 in HEK293/hERα and 122.0% of that of E2 in HEK293/hERβ. Strikingly, **3** showed no agonist potency for ERα or ERβ. These findings strongly suggest that **3** can inhibit L-Glu transporters without interaction with ERs.

In this study, we examined the potential of Tam-related compounds to inhibit GLAST/EAAT1 and GLT1/EAAT2, which are major astrocytic L-Glu transporters in the rat

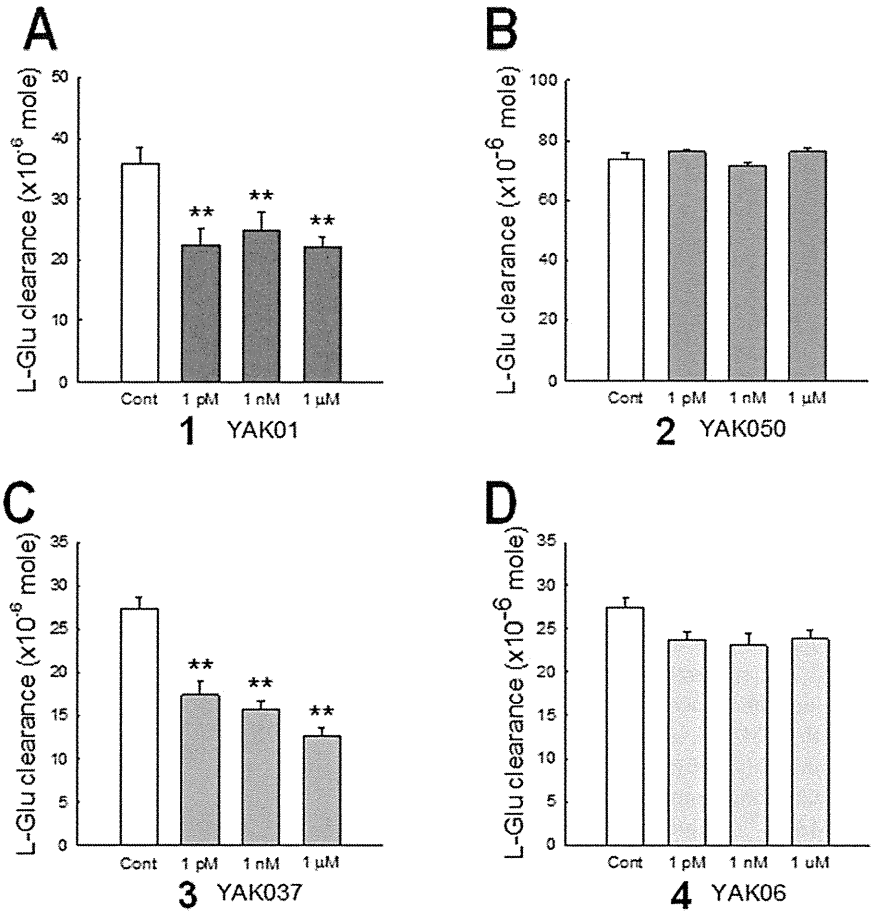

Figure 2. Compounds **1** and **3** inhibited L-Glu clearance in cultured astrocytes. The open column shows the control clearance, and colored columns show the clearance in the presence of various concentrations of compounds **1** (A), **2** (B), **3** (C), and **4** (D). $^{**}p < 0.01$ vs control group ($N = 6$), Tukey's test following ANOVA.

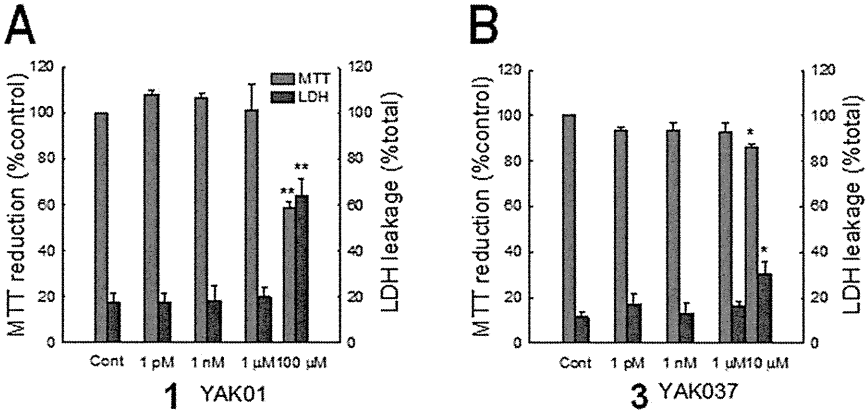

Figure 3. Effects of compounds **1** and **3** on cell viability. The results of MTT reduction and LDH leakage assays of **1** (A) and **3** (B) are shown. $^{*}p < 0.05$, $^{**}p < 0.01$ vs control group ($N = 6$), Tukey's test following ANOVA.

forebrain. Although GLT-1 is the main regulator of synaptically released L-Glu in vivo, the predominant subtype changes to GLAST in cultured astrocytes, possibly owing to the lack of interaction of astrocytes with neurons.[15] We confirmed that GLAST is the main functional L-Glu transporter in our primary-cultured astrocytes by Western blotting and pharmacological experiments (data not shown), in accordance with a previous report.[16] Therefore, the effects of the compounds observed here can be interpreted as being due to modulation of GLAST functional activity.

There is growing evidence that ERα, which is a nER that mediates genomic effects, can also be translocated to plasma membranes and mediate acute nongenomic effects in some cases. Transfection of CHO cells with nERs was reported to result in ER expression in both nuclei and membranes.[17] ERs on the plasma membranes of tumor cells were demonstrated to be structurally similar to nERs.[18] Further, mERα activated metabotropic glutamate receptor 5 (mGluR5) in striatal neurons in the CNS.[19] In our previous study, we clarified that the predominant ER subtype in cultured astrocytes was ERα, and

dx.doi.org/10.1021/cn200091w | ACS Chem. Neurosci. 2012, 3, 105–113

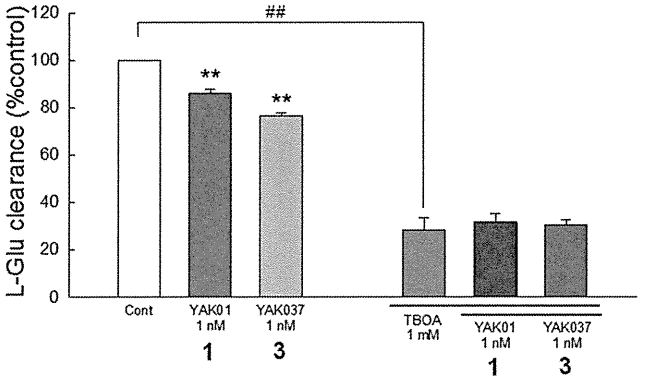

Figure 4. Compounds **1** and **3** suppressed L-Glu clearance in astrocyte culture by decreasing the functional activity of L-Glu transporter. L-Glu clearance in the presence and absence of compounds **1** and **3** is shown, together with their effects in the copresence of the potent nonselective L-Glu transporter inhibitor TBOA. $^{**}p < 0.01$ vs control group ($N = 6$), Tukey's test following ANOVA.

estrogens (such as E2 and Tam) inhibited L-Glu transporter activity via the activation of mERα.[5] We found that the effects of **1** were blocked by ICI182,780, suggesting an interaction of **1** with ERα. In addition, our pharmacological experiments showed that activation of both of MAPK and PI3K is necessary for the L-Glu transporter-inhibitory activity of **1**. There are many reports indicating that nongenomic effects involving mERα are mediated via MAPK[19−21] and PI3K.[20,22] Taken together, the effects of **1** may be mediated by mERα in a similar manner to E2 and Tam. E2 was reported to activate MAPK via both PI3K-dependent and independent pathways in a single neuron.[20] Whether or not the same signaling pathways also exist in astrocytes is not yet known. It is of interest that other studies have found that estrogens also inhibit dopamine transporter (DAT) through the activation of mERα.[23,24]

On the other hand, the effect of **3** was ER-independent and MAPK-independent, but PI3K-dependent. Our binding assay revealed that **1** binds with ERs, but **3** does not. Based on these results, we propose that the mechanisms of the L-Glu

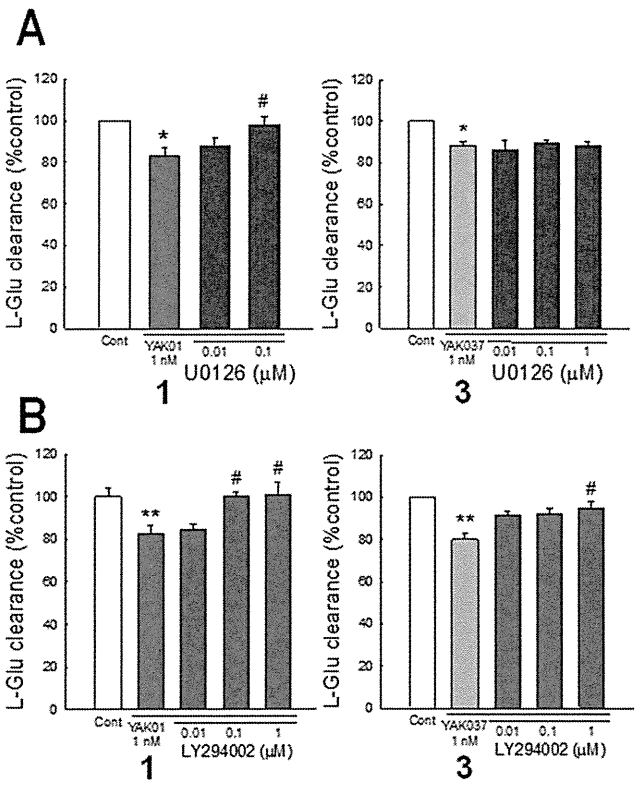

Figure 6. Involvement of MAPK and PI3K in the L-Glu transporter-inhibitory activity of compounds **1** (A) and **3** (B). Effects of compounds **1** (left panels) and **3** (right panels) on L-Glu clearance in the presence and absence of various concentrations of U0126, an inhibitor of MAPK/ERKs (A) or LY294002, a specific inhibitor of PI3K (B). $^{*}P < 0.05$, $^{**}p < 0.01$ vs control group, $\#p < 0.05$ vs compound-treated group ($N = 6$), Tukey's test following ANOVA.

transporter-inhibitory effects of **1** and **3** are different, as illustrated in Figure 8. The effect of **3** was possibly mediated by GPR30, a newly found ER, which is suggested to mediate the rapid nongenomic effects of estrogens.[25,26] In the case of GPR30, ICI182,780 acts as agonist, leading to activation of

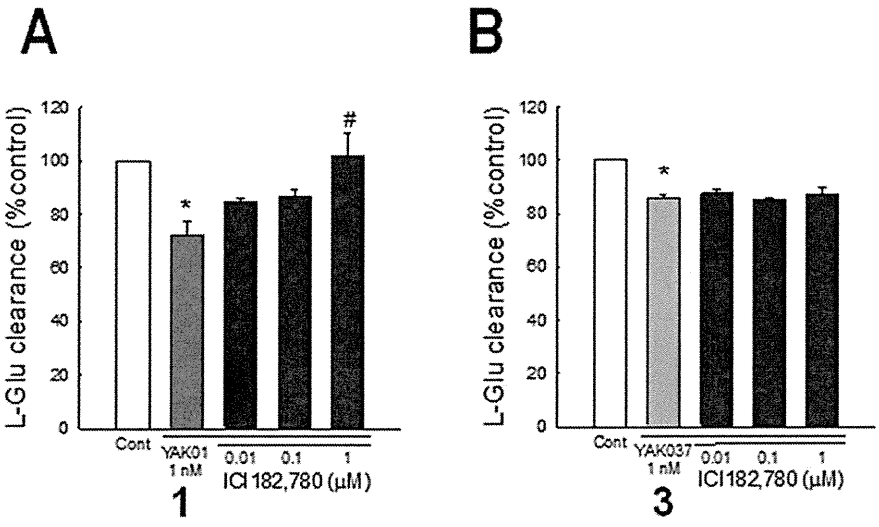

Figure 5. Involvement of ERs in the L-Glu transporter-inhibitory effects of compounds **1** and **3**. Effects of compounds **1** (A) and **3** (B) on L-Glu clearance in the presence and absence of various concentrations of ICI182,780, a high-affinity antagonist of ERs. $^{*}P < 0.05$ vs control group, $\#p < 0.05$ vs compound-treated group ($N = 6$), Tukey's test following ANOVA.

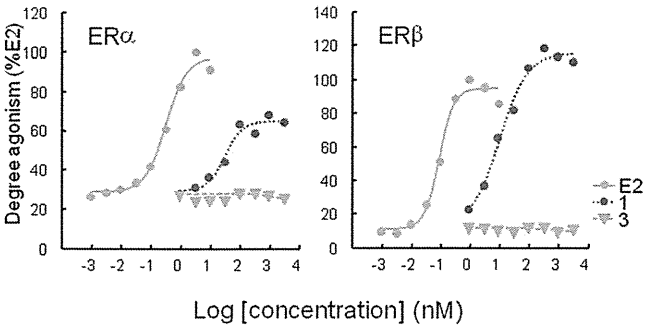

Figure 7. ER agonist potency of compounds **1** and **3** to nERs: dose dependence of binding of compounds **1** and **3** in HEK293/hERα cells (left) or HEK293/hERβ cells (right). Compound 1 showed dose-dependent agonist activity in both of HEK293/hERα cells (left) and HEK293/hERβ cells (right), though 3 showed no agonist potency for ERα or ERβ.

signal transduction pathways in a similar manner to estrogens.[27,28] However, we could not detect any effects of ICI182,780 alone on L-Glu transporter in our experiments (data not shown). In addition, Kuo et al. reported that GPR30 in astrocytes is detected not in the cell membranes but in the smooth endoplasmic reticulum,[29] while the cellular localization of GPR30 has been still controversially argued. In these contexts, GPR30 is an unlikely mediator to block the L-Glu transporters by the action of **3**.

According to Kisanga et al., the concentration of Tam in serum during conventional treatment for breast cancer (1–20 mg daily) is in the range from 20 to 225 nM.[30] Because **3** is more hydrophobic than Tam (the values of clogP for Tam and **3** are 7.56 and 9.70, respectively), it should exhibit greater permeability into the brain. Although other L-Glu transporter inhibitors, mainly L-Glu/aspartate analogues, are known, few of them have high brain transfer rates. Therefore, **3** is expected to be useful for biological research, and is also considered to be a promising candidate or lead compound for pharmacological application.

In conclusion, examination of several Tam-inspired compounds led to the discovery of two compounds that inhibited astrocytic L-Glu transporters at picomolar concentration. The inhibitory activity of compound **1** was mediated through the ER-MAPK/PI3K pathway, like that of Tam, though its transactivation activity was drastically reduced as compared with E2. In contrast, the inhibitory effect of **3** was manifested through an ER-independent and MAPK-independent, but PI3K-dependent pathway, and **3** showed no transactivation activity. These results suggest that **3** may represent a new platform for the development of novel L-Glu transporter inhibitors with higher brain transfer rates and reduced adverse effects.

METHODS

Chemistry. *General Procedures.* All reagents were commercial products and were used without further purification, unless otherwise noted. NMR data were recorded on a JEOL-400 or a Bruker Avance 400 NMR spectrometer (400 MHz for ^{1}H NMR and 100 MHz for ^{13}C NMR). *d*-$CDCl_3$ was used as a solvent, unless otherwise noted. Chemical shifts (δ) are reported in ppm with respect to internal tetramethylsilane (δ = 0 ppm) or undeuterated residual solvent (i.e., $CHCl_3$ (δ = 7.265 ppm)). Coupling constants are given in hertz. Coupling patterns are indicated as follows: m = multiplet, d = doublet, s = singlet, br = broad. High-resolution mass spectrometry (HRMS) was conducted in the electron spray ionization (ESI)-time-of-flight

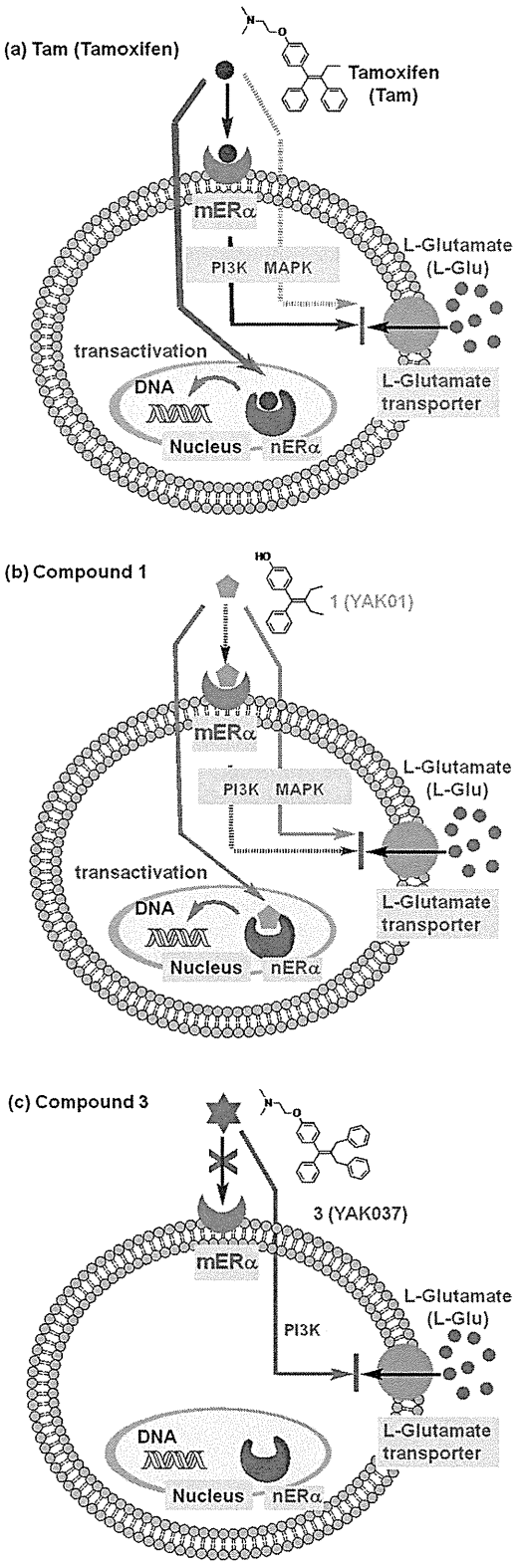

Figure 8. Schematic illustration of the proposed mechanisms of the effects of tamoxifen (a) and compounds **1** (b) and **3** (c).

(TOF) detection mode on a Bruker micrOTOF-05. FAB-MS and high-resolution FAB-MS were obtained on a JMS700-MSTATION (JEOL, Japan). Column chromatography was carried out on silica gel (silica gel 60N (100–210 μm), Kanto Chemicals, Japan). Flash column chromatography was performed on silica gel H (Merck, Germany). Analytical thin-layer chromatography (TLC) was performed on

precoated plates of silica gel HF_{254} (Merck, Germany). All the melting points were measured with a Yanaco Micro Melting Point apparatus and are uncorrected. Combustion analyses were carried out in the microanalysis laboratory of this faculty.

Synthesis of Compounds. Compounds **1** and **2** were synthesized from 4-hydroxybenzophenone and butyl-3-one or dibenzylacetone by using $TiCl_4$ in the presence of Zn. Introduction of the *N,N*-dimethylaminoethyl moiety at the phenolic hydroxyl group of **1** and **2** was carried out by base treatment, followed by addition of 2-dimethylaminoethyl chloride hydrochloride.

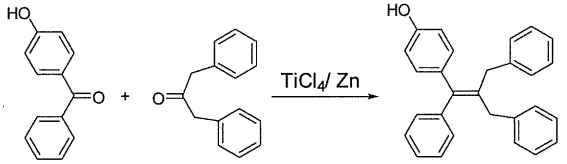

2 (YAK050)

Synthesis of Tamoxifen-Related Compounds. Compound 2 (YAK050). To a suspension of Zn powder (916.6 mg; 6.9 equiv with respect to 4-hydroxybenzophenone) in dry THF (30 mL) in a 200 mL three-necked flask, $TiCl_4$ (0.61 mL, 2.8 equiv) was added dropwise under an argon atmosphere at −20 °C (in an ice-salt bath) over 2 min. The resulting light green-yellow mixture was stirred at −20 °C for 20 min and then the cooling bath was removed. After 20 min, the flask was immersed in a preheated oil bath at 100 °C and refluxed at 100 °C with stirring for 2.5 h. To the resulting deep blue mixture was added in one portion a solution of 4-hydroxybenzophenone (401.3 mg, 2.02 mmol) and dibenzyl ketone (1.2735 g, 3 equiv) in 50 mL of dry THF. The resultant mixture was heated at reflux at 100 °C with stirring for 2 h, then allowed to cool to rt, and poured into 400 mL of 0.5 N aqueous NaOH solution. The whole was extracted with ethyl acetate (500 mL). The organic layer was washed with water, dried over $MgSO_4$ and evaporated to give a pale yellow oil (1.5172 g), which was column-chromatographed (silica gel, acetone/*n*-hexane (1:7)) to give 365.0 mg (48% yield) of the olefin **2** as a white amorphous solid. Mp: 57–60 °C. ^{1}H NMR ($CDCl_3$): δ: 7.287–7.079 (m, 17H), 6.760 (d, 2H, J = 8.8 Hz), 4.792 (s, 1H), 3.413 (s, 2H), 3.377 (s, 2H). ^{13}C NMR ($CDCl_3$): δ: 154.1, 143.0, 140.7, 140.4, 135.8, 135.4, 130.7, 129.4, 128.8, 128.3, 128.3, 128.2, 126.5, 125.9, 115.1, 37.4, 37.2. HRMS (ESI^-): Calcd. for $C_{28}H_{23}O$ ($[M - H]^-$), 375.1754. Found: 375.1744. Anal. Calcd for $C_{28}H_{24}O{\cdot}0.2H_2O$: C, 88.48; H, 6.47; N, 0.00. Found: C, 88.36; H, 6.63; N, 0.00.

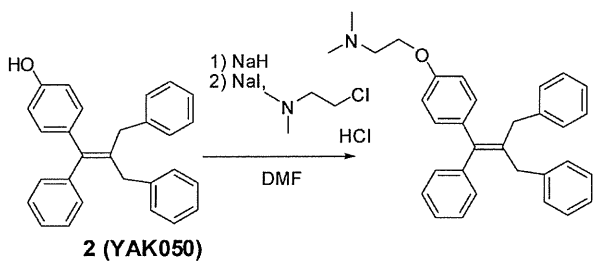

2 (YAK050)

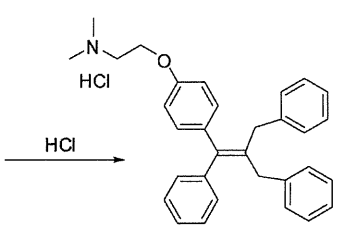

3 (YAK037)

Compound 3 (YAK037). To a suspension of NaH (60%, 42 mg, 1.05 mmol) in DMF (3 mL) at 0 °C was added a solution of the phenol **2** (158.2 mg, 0.420 mmol) in DMF (3 mL). The reaction mixture was stirred for 30 min at 0 °C, and then a solution of 2-dimethylaminoethyl chloride hydrochloride (181.0 mg, 1.256 mmol, 3.0 equiv) and NaI (94.0 mg, 0.627 mmol, 1.5 equiv) in DMF (3 mL) was added. The reaction mixture was stirred at 50 °C for 30 min, and then saturated aqueous NH_4Cl was added to quench the reaction. The mixture was extracted with Et_2O. The organic layer was washed with brine, dried over Na_2SO_4 and evaporated to afford a residue, which was column-chromatographed (ethyl acetate/Et_3N = 100/1) to give the intermediate amine (83.0 mg, 44% yield). The HCl salt of the resultant amine was prepared by repeated addition of a solution of 2 N HCl in Et_2O to a solution of the amine in ethyl acetate, followed by evaporation of the organic solvent to give **3**.

3: White solid. Mp. 169–170 °C. ^{1}H NMR ($CDCl_3$): δ: 13.073 (brs, 1H), 7.306–7.195 (m, 13H), 7.102–7.074 (m, 4H), 6.832 (d, 2H, J = 8.8 Hz), 4.481–4.459 (m, 2H), 3.425–3.390 (m, 6H), 2.893 (s, 6H). ^{13}C NMR ($CDCl_3$) δ: 155.7, 142.8, 140.4, 140.3, 140.2, 136.8, 136.2, 130.9, 129.4, 128.8, 128.7, 128.4, 128.3, 128.3, 126.6, 126.0, 125.9, 114.3, 62.8, 56.5, 43.6, 37.4, 37.2. HRMS (ESI^+, $[M + H]^+$): Calcd. for $C_{32}H_{34}NO$, 448.26349. Found: 448.26092. Anal. Calcd for $C_{32}H_{34}ClNO{\cdot}1/4H_2O$: C, 78.67; H, 7.12; N, 2.87. Found: C, 78.64; H, 7.30; N, 2.87.

Compound 1 (YAK01).

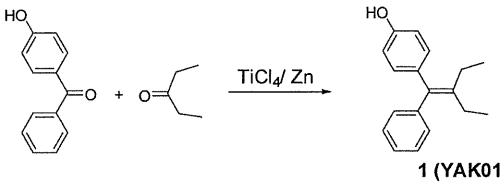

1 (YAK01)

To a suspension of Zn (0.86 g, 13.2 mmol) in 30 mL of dry THF at −5 °C was added dropwise $TiCl_4$ (0.72 mL, 6.6 mmol) under an argon atmosphere. The mixture was heated at reflux for 2 h. A solution of 4-hydroxybenzophenone (341.1 mg, 1.7 mmol) and 3-pentanone (0.50 mL, 5.0 mmol) in 50 mL of dry THF was added in one portion, and heating was continued at reflux for 6 h. Then the reaction mixture was cooled to rt, quenched with 10% aqueous K_2CO_3 (100 mL) and extracted with ethyl acetate (3 × 80 mL). The combined organic phase was washed with brine (50 mL), dried over Na_2SO_4, and evaporated to give a residue, which was flash column-chromatographed (3:1 hexane/ethyl acetate) to afford **1** (383.4 mg, 88.3%) as a white solid.

1: Mp. 76.0–76.5 °C (colorless needles, recrystallized from *n*-hexane). ^{1}H NMR ($CDCl_3$) δ: 7.261 (2H, t, J = 8.0 Hz), 7.173 (1H, d, J = 7.2 Hz), 7.128 (2H, d, J = 7.6 Hz), 7.009 (2H, d, J = 8.8 Hz), 6.726 (2H, d, J = 8.8 Hz), 4.763 (1H, s), 2.152 (2H, quartet, J = 7.6 Hz), 2.115 (2H, quartet, J = 6.0 Hz), 1.007 (3H, t, J = 7.6 Hz), 0.994 (3H, t, J = 7.6 Hz). ^{13}C NMR ($CDCl_3$) δ: 153.7, 143.7, 142.0, 136.5, 136.2, 130.5, 129.2, 127.9, 125.9, 114.8, 24.4, 24.3, 13.3. HRMS (ESI^-, $[M - H]^-$): Calcd. for $C_{18}H_{19}O^-$, 251.14414. Found: 251.14730. HRMS (FAB-MS, $[M]^+$) Calcd. for $C_{18}H_{20}O$, 252.1514. Found: 252.1528. Anal. Calcd. for $C_{18}H_{20}O$: C, 85.67; H, 7.99; N, 0.00. Found: C, 85.38; H, 8.13; N, 0.00.

Compound 4 (YAK06).

2-Dimethylaminoethyl chloride hydrochloride (282.4 mg, 2.0 mmol) and K_2CO_3 (1.5734 g, 11.4 mmol) were stirred in acetone/H_2O (18 mL/2 mL) at 0 °C for 30 min, then compound **1** (139.1 mg, 0.55 mmol) and K_2CO_3 (421.1 mg, 3.1 mmol) were added, and the whole was heated at reflux for 24 h, then cooled to rt. Inorganic materials were removed by filtration, and the filtrate was evaporated. The residue was flash column-chromatographed (100:1 ethyl acetate/Et_3N) to afford the amine as a white solid (88.0 mg). To a solution of the amine in ethyl acetate, a solution of HCl in ether was added to give a precipitate, which was collected and recrystallized from ethanol/ethyl acetate to give **4** (95.0 mg, 48%) as a white powder. **4**: Mp. 129.5–130.2 °C. ^{1}H NMR ($CDCl_3$) δ 726–6.90 (9H, m), 4.07 (2H, t, J = 6.0 Hz), 2.75 (2H, t, J = 6.0 Hz), 2.40 (6H, s), 2.15 (4H, d, J = 7.2 Hz), 1.00 (6H, t, J = 7.2 Hz). HRMS (FAB-MS, $[M\text{-}Cl]^+$): Calcd. for $C_{22}H_{30}NO^+$: 324.2322. Found: 324.2321.

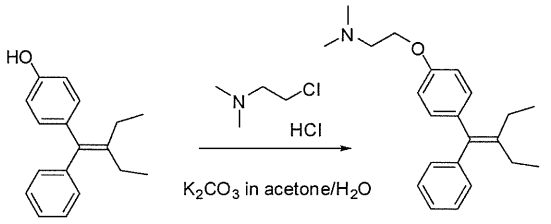

1 (YAK01)

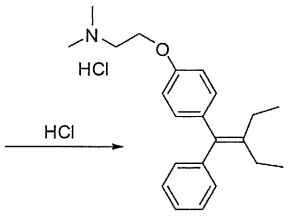

4 (YAK06)

Biology. All procedures using live animals in this study were conducted in accordance with the guidelines of the National Institute of Health Sciences, Japan.

Materials. Dulbecco's modified Eagle's medium (DMEM) and fetal bovine serum (FBS) were purchased from GIBCO (CA, USA). Glutamate dehydrogenase (GLD) was purchased from Roche (Mannheim, Germany). β-Nicotinamide adenine dinucleotide (βNAD), 3-(4,5-dimethyl-2-thiazolyl)-2,5-diphenyl-2H-tetrazolium bromide (MTT), 1-methoxy-5-methylphenazinium methyl sulfate (MPMS), lactate lithium salt and LY294002 were purchased from Sigma (MO, USA). DL-threo-β-benzyloxyaspartic acid (TBOA) and ICI182,780 were purchased from Tocris (MO, USA). U0126 was purchased from Promega (WI, USA). Assay kits for hormonal effects on HEK293/hERα and HEK293/hERβ reporter cells were purchased from Clontech (CA, USA).

Cell Culture. Primary cultures of astrocytes were prepared from the cerebral cortices of 3-day-old neonates of Wistar rats, as described previously.[31] Briefly, dissociated cortical cells were suspended in modified DMEM containing 30 mM glucose, 2 mM glutamine, 1 mM pyruvate and 10% FBS, and plated on uncoated 75 cm^2 flasks at the density of 600 000 cells/cm^2. A monolayer of type I astrocytes was obtained 12−14 days after plating. Nonastrocytes such as microglia were detached from the flasks by shaking and removed by changing the medium. Astrocytes in the flasks were dissociated by trypsinization, reseeded on uncoated 96-well microtiter plates at 20 000 cells/cm^2, and incubated until the cells became confluent (approximately 9−10 days after reseeding). In this culture, >98% of the cells were identified as type I astrocytes on the basis of positivity for GFAP and flattened, polygonal appearance.

Measurement of Extracellular L-Glu Concentration. Extracellular L-Glu concentration was measured by means of a colorimetric method according to Abe et al.[32] Briefly, 50 μL of culture supernatant was transferred to each well of a 96-well microtiter plate and mixed with 50 μL of substrate mixture consisting of 20 U/mL GLD, 2.5 mg/mL β-NAD, 0.25 mg/mL MTT, 100 μM MPMS and 0.1% (v/v) Triton X-100 in 0.2 M Tris-HCl buffer (pH 8.2). After 10 min incubation at 37 °C, the reaction was stopped by adding 100 μL of solution containing 50% (v/v) dimethylformamide and 20% (wt/vol) SDS (pH 4.7). In this reaction, MTT (yellow) is converted into MTT formazan (purple) in proportion to the L-Glu concentration. The amount of MTT formazan was determined by measuring the absorbance at 570 nm (test wavelength) and 655 nm (reference wavelength) with a microplate reader. The concentration of L-Glu was estimated from a standard curve, which was constructed in each assay using cell-free medium containing known concentrations of L-Glu. L-Glu clearance was shown as the amount of L-Glu taken up by astrocytes, which was calculated from the concentration difference in the medium.

Treatment with Test Compounds. L-Glu was dissolved at 1 mM in phosphate-buffered saline and diluted to 100 μM with the culture medium. Compounds **1**, **2**, **3**, and **4** were dissolved at 100, 100, 100, and 10 mM, respectively, in dimethyl sulfoxide (DMSO) and diluted to the required final concentrations with the culture medium. The concentration of DMSO in the medium was controlled to be below 0.1%, because we had already confirmed that 0.1% DMSO has no effect on L-Glu transport activity or cell viability (data not shown). Cells were incubated with test compounds for 24 h. TBOA (IC50 = 48 μM for GLAST, 7 μM for GLT1) was freshly dissolved at 1 mM in culture medium for each experiment. ICI182,780 (IC50 = 0.29 nM for ERs), U0126 (IC50 = 72 nM for MEK1, 58 nM for MEK2), and LY294002 (IC50 = 1 μM for class 1 PI3K, 19 μM for class 2 PI3K) were dissolved at 1, 5, and 5 mM, respectively, in DMSO, and the solutions were diluted with culture medium to yield the required final concentrations. These inhibitors were coapplied with 1 nM test compounds (**1**−**4**) for 24 h.

Assay Procedure for Hormonal Effects on HEK293/hERα and HEK293/hERβ Reporter Cells. Human embryo kidney 293 cells (HEK293) were grown in FBS (+) DMEM in 100 mm dishes. Cells were subcultured once or twice a week at about 80% confluence. A solution of 12.4 μL of 2 M calcium ion, 100 ng/well reporter or negative control vector (pERE-TA-SEAP or pTA-SEAP, Clontech), 50 ng/well expression vector (pcDNA3 ERα or pcDNA3 ERβ, generous gift from Dr. Shige-aki Kato, University of Tokyo, Japan), and 100 ng/well positive control vector (pSV-β-galactosidase, Promega) was diluted to a final volume of 10 μL/well. This mixture was carefully added dropwise to the same volume of HEPES solution with slow vortexing, and the mixture was incubated at rt for 20 min to obtain a precipitate. Cells from the exponential growth phase were seeded (3.0×10^4 cells/ml) into 96-well plates the day before transfection. The cells were incubated with fresh medium for 1 h, then 1/10 volume of precipitate was added to each well and incubation was continued for 24 h at 37 °C in an atmosphere of 5% CO_2 in air. The medium was replaced with fresh FBS (-) medium and incubation was continued for a further 24 h. Then the cells were incubated with test compounds for 24 h at 37 °C in an atmosphere of 5% CO_2 in air. SEAP activity (Great EscapeTM SEAP chemiluminescence kit 2.0, Clontech) and β-galactosidase activity (β-Galactosidase Enzyme Assay System with Reporter Lysis Buffer, Promega) were measured with a Spectramax M5 microplate reader (Molecular Devices Japan, Tokyo, Japan). All transfections were performed in triplicate.

Statistical Analysis. Data were obtained from four independent experiments (averaged values of six wells for each) unless otherwise noted. Data are expressed as means ± SEM of these data. Tests of homogeneity of variance, normality, and distribution were performed to ensure that the assumptions required for standard parametric ANOVA were satisfied. Statistical analysis was performed by one-way repeated-measures ANOVA with post hoc Tukey's test for multiple pairwise comparisons.

AUTHOR INFORMATION

Corresponding Author

*(K.S.) Telephone and Fax: +81-3-3700-9698. E-mail: kasato@nihs.go.jp. (T.O.) Telephone: +81-3-5840-4730. Fax: +81-3-5840-4735. E-mail: ohwada@mol.f.u-tokyo.ac.jp.

Author Contributions

†These two authors equally contributed to this Article. Individual author contributions: K.S. designed the biological experimental plan, performed biological experiments, data analysis, manuscript writing and preparation. J.K. and Y.S. performed experimental work. K.T. contributed to the data analysis. J.O., K.N. and Y.S. provided advice on the experimental direction. Y.O. carried out organic synthesis, data analysis and wrote portions of the manuscript. Y.S. carried out organic synthesis. T.O. designed and oversaw all organic chemistry studies, carried out organic synthesis and also performed data analysis and manuscript writing and preparation.

Funding

This work was partly supported by a Grant-in-Aid from the Food Safety Commission, Japan (No. 1003), a Grant-in-Aid for Young Scientists from MEXT, Japan (KAKENHI 21700422), the Program for Promotion of Fundamental Studies in Health Sciences of NIBIO, Japan, a Health and Labor Science Research Grant for Research on Risks of Chemicals, a Health and Labor Science Research Grant for Research on New Drug Development from MHLW, Japan, awarded to K.S., and a Health and Labor Science Research Grant for Research on Risks of Chemicals from MHLW, Japan, awarded to K.N. and T.O.

Notes

The authors declare no competing financial interest.

■ ACKNOWLEDGMENTS

We thank Dr. Shige-aki Kato for providing pcDNA3 hERα and pcDNA3 hERβ.

■ ABBREVIATIONS

βNAD; β-nicotinamide adenine dinucleotide; CNS; central nervous system; DMEM; Dulbecco's modified Eagle's medium; DMSO; dimethyl sulfoxide; E2; 17β-estradiol; ESI; electron spray ionization; FBS; fetal bovine serum; GLD; glutamate dehydrogenase; HEK-293; Human embryo kidney 293 cells; HRMS; high-resolution mass spectrometry; L-Glu; L-glutamate; MAPK; mitogen-activated protein kinase; MEK; mitogen-activated protein kinase/extracellular signal-regulated kinase; mERα; membrane-associated estrogen receptor α; mGluR5; metabotropic glutamate receptor 5; MPMS; 1-methoxy-5-methylphenazinium methyl sulfate; MTT; 3-(4,5-dimethyl-2-thiazolyl)-2,5-diphenyl-2H-tetrazolium bromide; nERs; nuclear estrogen receptors; PI3K; phosphatidylinositol 3-kinase; Tam; tamoxifen; TBOA; DL-threo-β-benzyloxyaspartic acid; TLC; thin-layer chromatography; TOF; time-of-flight

■ REFERENCES

(1) Kumar, A., Singh, R. L., and Babu, G. N. (2010) Cell death mechanisms in the early stages of acute glutamate neurotoxicity. *Neurosci. Res. 66*, 271–278.

(2) Choi, D. W. (1988) Glutamate neurotoxicity and diseases of the nervous system. *Neuron 1*, 623–634.

(3) Logan, W. J., and Snyder, S. H. (1971) Unique high affinity uptake systems for glycine, glutamic and aspartic acids in central nervous tissue of the rat. *Nature 234*, 297–299.

(4) Beart, P. M., and O'Shea, R. D. (2007) Transporters for L-glutamate: an update on their molecular pharmacology and pathological involvement. *Br. J. Pharmacol. 150*, 5–17.

(5) Sato, K., Matsuki, N., Ohno, Y., and Nakazawa, K. (2003) Estrogens inhibit L-glutamate uptake activity of astrocytes via membrane estrogen receptor alpha. *J. Neurochem. 86*, 1498–1505.

(6) Olivier, S., Close, P., Castermans, E., de Leval, L., Tabruyn, S., Chariot, A., Malaise, M., Merville, M. P., Bours, V., and Franchimont, N. (2006) Raloxifene-induced myeloma cell apoptosis: a study of nuclear factor-kappaB inhibition and gene expression signature. *Mol. Pharmacol. 69*, 1615–1623.

(7) Sato, K., Saito, Y., Oka, J., Ohwada, T., and Nakazawa, K. (2008) Effects of tamoxifen on L-glutamate transporters of astrocytes. *J. Pharmacol. Sci. 107*, 226–230.

(8) Bunch, L., Erichsen, M. N., and Jensen, A. A. (2009) Excitatory amino acid transporters as potential drug targets. *Expert Opin. Ther. Targets 13*, 719–731.

(9) Margueron, R., Duong, V., Bonnet, S., Escande, A., Vignon, F., Balaguer, P., and Cavailles, V. (2004) Histone deacetylase inhibition and estrogen receptor alpha levels modulate the transcriptional activity of partial antiestrogens. *J. Mol. Endocrinol. 32*, 583–594.

(10) Thompson, D. S., Spanier, C. A., and Vogel, V. G. (1999) The relationship between tamoxifen, estrogen, and depressive symptoms. *Breast J. 5*, 375–382.

(11) Grilli, S. (2006) Tamoxifen (TAM): the dispute goes on. *Ann. Ist. Super. Sanita 42*, 170–173.

(12) Sha, Y., Tashima, T., Mochizuki, Y., Toriumi, Y., Adachi-Akahane, S., Nonomura, T., Cheng, M., and Ohwada, T. (2005) Compounds structurally related to tamoxifen as openers of large-conductance calcium-activated K^+ channel. *Chem. Pharm. Bull. (Tokyo) 53*, 1372–1373.

(13) Robertson, D. W., Katzenellenbogen, J. A., Long, D. J., Rorke, E. A., and Katzenellenbogen, B. S. (1982) Tamoxifen antiestrogens. A comparison of the activity, pharmacokinetics, and metabolic activation of the cis and trans isomers of tamoxifen. *J. Steroid Biochem. 16*, 1–13.

(14) Weltje, L., vom Saal, F. S., and Oehlmann, J. (2005) Reproductive stimulation by low doses of xenoestrogens contrasts with the view of hormesis as an adaptive response. *Hum. Exp. Toxicol. 24* (9), 431–437.

(15) Perego, C., Vanoni, C., Bossi, M., Massari, S., Basudev, H., Longhi, R., and Pietrini, G. (2000) The GLT-1 and GLAST glutamate transporters are expressed on morphologically distinct astrocytes and regulated by neuronal activity in primary hippocampal co-cultures. *J. Neurochem. 75*, 1076–1084.

(16) Guillet, B., Lortet, S., Masmejean, F., Samuel, D., Nieoullon, A., and Pisano, P. (2002) Developmental expression and activity of high affinity glutamate transporters in rat cortical primary cultures. *Neurochem. Int. 40*, 661–671.

(17) Razandi, M., Pedram, A., Greene, G. L., and Levin, E. R. (1999) Cell membrane and nuclear estrogen receptors (ERs) originate from a single transcript: studies of ERalpha and ERbeta expressed in Chinese hamster ovary cells. *Mol. Endocrinol. 13*, 307–319.

(18) Pappas, T. C., Gametchu, B., and Watson, C. S. (1995) Membrane estrogen receptors identified by multiple antibody labeling and impeded-ligand binding. *FASEB J. 9*, 404–410.

(19) Grove-Strawser, D., Boulware, M. I., and Mermelstein, P. G. (2010) Membrane estrogen receptors activate the metabotropic glutamate receptors mGluR5 and mGluR3 to bidirectionally regulate CREB phosphorylation in female rat striatal neurons. *Neuroscience 170*, 1045–1055.

(20) Mannella, P., and Brinton, R. D. (2006) Estrogen receptor protein interaction with phosphatidylinositol 3-kinase leads to activation of phosphorylated Akt and extracellular signal-regulated kinase 1/2 in the same population of cortical neurons: a unified mechanism of estrogen action. *J. Neurosci. 26*, 9439–9447.

(21) Szego, E. M., Barabas, K., Balog, J., Szilagyi, N., Korach, K. S., Juhasz, G., and Abraham, I. M. (2006) Estrogen induces estrogen receptor alpha-dependent cAMP response element-binding protein phosphorylation via mitogen activated protein kinase pathway in basal forebrain cholinergic neurons in vivo. *J. Neurosci. 26*, 4104–4110.

(22) Vasudevan, N., Kow, L. M., and Pfaff, D. (2005) Integration of steroid hormone initiated membrane action to genomic function in the brain. *Steroids 70*, 388–396.

(23) Alyea, R. A., Laurence, S. E., Kim, S. H., Katzenellenbogen, B. S., Katzenellenbogen, J. A., and Watson, C. S. (2008) The roles of membrane estrogen receptor subtypes in modulating dopamine transporters in PC-12 cells. *J. Neurochem. 106* (4), 1525–1533.

(24) Watson, C. S., Alyea, R. A., Hawkins, B. E., Thomas, M. L., Cunningham, K. A., and Jakubas, A. A. (2006) Estradiol effects on the dopamine transporter - protein levels, subcellular location, and function. *J. Mol. Signaling 1*, 5.

(25) Filardo, E. J., and Thomas, P. (2005) GPR30: a seven-transmembrane-spanning estrogen receptor that triggers EGF release. *Trends. Endocrinol. Metab. 16* (8), 362–367.

(26) Revankar, C. M., Cimino, D. F., Sklar, L. A., Arterburn, J. B., and Prossnitz, E. R. (2005) A transmembrane intracellular estrogen receptor mediates rapid cell signaling. *Science 11;307* (5715), 1625–1630.

(27) Filardo, E. J., Quinn, J. A., Bland, K. I., and Frackelton, A. R. Jr. (2000) Estrogen-induced activation of Erk-1 and Erk-2 requires the G

protein-coupled receptor homolog, GPR30, and occurs via transactivation of the epidermal growth factor receptor through release of HB-EGF. *Mol. Endocrinol. 14* (10), 1649–1660.

(28) Thomas, P., Pang, Y., Filardo, E. J., and Dong, J. (2005) Identity of an estrogen membrane receptor coupled to a G protein in human breast cancer cells. *Endocrinology 146* (2), 624–632.

(29) Kuo, J., Hamid, N., Bondar, G., Prossnitz, E. R., and Micevych, P. (2010) Membrane estrogen receptors stimulate intracellular calcium release and progesterone synthesis in hypothalamic astrocytes. *J. Neurosci. 30* (39), 12950–12957.

(30) Kisanga, E. R., Gjerde, J., Guerrieri-Gonzaga, A., Pigatto, F., Pesci-Feltri, A., Robertson, C., Serrano, D., Pelosi, G., Decensi, A., and Lien, E. A. (2004) Tamoxifen and metabolite concentrations in serum and breast cancer tissue during three dose regimens in a randomized preoperative trial. *Clin. Cancer Res. 10*, 2336–2343.

(31) Suzuki, K., Ikegaya, Y., Matsuura, S., Kanai, Y., Endou, H., and Matsuki, N. (2001) Transient upregulation of the glial L-glutamate transporter GLAST in response to fibroblast growth factor, insulin-like growth factor and epidermal growth factor in cultured astrocytes. *J. Cell Sci. 114*, 3717–3725.

(32) Abe, K., Abe, Y., and Saito, H. (2000) Evaluation of L-glutamate clearance capacity of cultured rat cortical astrocytes. *Biol. Pharm. Bull. 23*, 204–207.

Chapter 10

Efficient Hepatic Differentiation from Human iPS Cells by Gene Transfer

Kenji Kawabata, Mitsuru Inamura, and Hiroyuki Mizuguchi

Abstract

Establishment of protocols for the differentiation of hepatic cells from human embryonic stem (ES) and induced pluripotent stem (iPS) cells could contribute to regenerative cell therapies or drug discovery and development. However, the differentiation efficiency of endoderm-derived cells, such as hepatic cells, from human ES and iPS cells is poor because hepatic cells are differentiated via multiple lineages including endodermal cells, hepatic progenitor cells, and mature hepatocytes. We show here the protocols for efficient hepatic differentiation from human ES and iPS cells by adenovirus vector-mediated gene transfer.

Key words: ES cells, iPS cells, Hepatocytes, Adenovirus vector, Regenerative medicine, Drug development

1. Introduction

In vertebrate development, the liver is derived from the primitive gut tube, which is formed by a flat sheet of cells called the definitive endoderm (1, 2). Afterward, the definitive endoderm is separated into the liver buds and differentiated into hepatoblasts. The hepatoblasts can differentiate into both mature hepatocytes and cholangiocytes. Each step of cell growth and differentiation is tightly regulated by intra- and extracellular signaling (3). Activin A, fibroblast growth factors (FGFs), bone morphogenic protein (BMP), hepatocyte growth factor (HGF), and oncostatin M (OSM) are the most essential extracellular signaling molecules. At the intracellular level, the liver-enriched transcription factors, i.e., hepatocyte nuclear factors (HNFs), CCAAT enhancer binding protein (C/EBP) α and β, and hematopoietically expressed homeobox (HEX), are required for the hepatic differentiation (4, 5). Among these

Takahiro Ochiya (ed.), *Liver Stem Cells: Methods and Protocols*, Methods in Molecular Biology, vol. 826,
DOI 10.1007/978-1-61779-468-1_10,

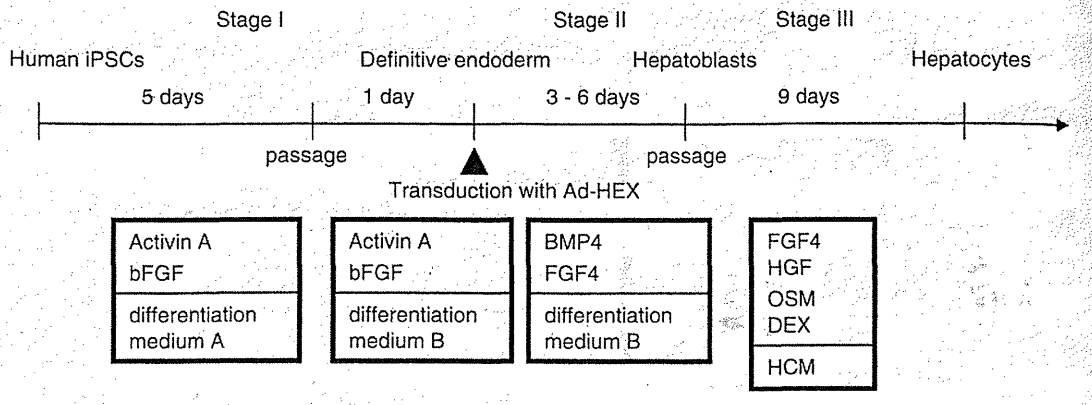

Fig. 1. A strategy for the differentiation of human iPS cells into hepatoblasts and hepatocytes. A schematic representation illustrating the procedure for differentiation of human iPS cells into hepatocytes is shown.

transcription factors, Hex is known to function at the earliest stage in hepatic differentiation (6). Targeted deletion of the HEX gene in the mouse results in embryonic lethality and a loss of the fetal liver parenchyma (7, 8). The hepatic genes, such as albumin, HNF4a, and prospero-related homeobox 1 (PROX1), are transiently expressed in the definitive endoderm of HEX-null embryos, and further morphogenesis of the hepatoblasts does not occur (9). Together, these findings underscore that HEX is essential for the definitive endoderm to adopt a hepatic cell fate.

Here, we show the protocol for the efficient differentiation of hepatoblasts from human ES and iPS cells. Our strategy is based on an imitation of in vivo liver development (Fig. 1). We have found that differentiation of hepatoblasts from the human ES and iPS cell-derived definitive endoderms, but not from undifferentiated human ES and iPS cells, could be facilitated by adenovirus (Ad) vector-mediated transient transduction of a HEX gene (10). Hepatoblasts derived from human iPS cells by HEX transduction were able to differentiate into functional hepatocytes in vitro. Furthermore, all the procedures for culture and differentiation were performed under serum/feeder cell-free chemically defined conditions. Our protocol based on Ad vector-mediated transient transduction under chemically defined conditions would provide a platform for drug screening as well as safe regenerative cell therapies.

2. Materials

2.1. Adenovirus Vectors

1. The human HEX cDNA (GenBank Accession No. BC014336) (Invitrogen, Carlsbad, CA).
2. Shuttle plasmid pHMEF5 (11).
3. Vector plasmid pAdHM41-K7 (12).

2.2. Cells

1. Human iPS cells (see Note 1).
2. Mitomycin C-inactivated mouse embryonic fibroblasts (MEF) (Hygro-Resistant Strain C57/BL6) (Millipore, Bedford, MA) (see Note 1).
3. HepG2 cells.

2.3. Medium and Growth Factors

1. Defined serum-free medium (hESF9): hESF-GRO medium (Cell Science & Technology Institute, Sendai, Japan) supplemented with 10 μg/ml human recombinant insulin, 5 μg/ml human apotransferrin, 10 μM 2-mercaptoethanol, 10 μM ethanolamine, 10 μM sodium selenite, oleic acid conjugated with fatty acid-free bovine albumin, 10 ng/ml bFGF, and 100 ng/ml heparin (all from Sigma, St. Louis, MO).
2. Laminin from the Engelbreth-Holm-Swarm murine sarcoma basement membrane (Sigma).
3. Twelve-well culture plate (Sumitomo Bakelite, Tokyo, Japan).
4. Laminin-coated tissue culture 12-well plate: Dilute laminin in PBS for a final dilution of 1:50. Add 1 ml of laminin solution to coat each well of a 12-well plate. Incubate the plates for 3–24 h at 37°C. Remove laminin solution and wash the well with PBS immediately before use.
5. Accutase (Invitrogen).
6. Differentiation medium A: hESF-GRO medium (Cell Science & Technology Institute) supplemented with 10 μg/ml human recombinant insulin, 5 μg/ml human apotransferrin, 10 μM 2-mercaptoethanol, 10 μM ethanolamine, 10 μM sodium selenite, and 0.5 mg/ml fatty acid-free bovine albumin (BSA) (Sigma).
7. bFGF (Sigma).
8. Activin A (R&D Systems, Minneapolis, MN).
9. Trypsin–EDTA: 0.0125% trypsin, 0.01325 mM EDTA (Invitrogen).
10. Trypsin inhibitor A: Differentiation medium A supplemented with 0.1% soybean trypsin inhibitor (Sigma).
11. Differentiation medium B: hESF-DIF (Cell Science & Technology Institute) medium supplemented with 10 μg/ml human recombinant insulin, 5 μg/ml human apotransferrin, 10 μM 2-mercaptoethanol, 10 μM ethanolamine, 10 μM sodium selenite, and 0.5 mg/ml fatty acid-free BSA.
12. FGF4 (R&D Systems).
13. BMP4 (R&D Systems).
14. Trypsin inhibitor B: Differentiation medium B supplemented with 0.1% soybean trypsin inhibitor (Sigma).
15. Hepatocyte culture medium (HCM) supplemented with SingleQuots (Lonza, Walkersville, MD).
16. HGF (R&D Systems).

Table 1
List of Taqman gene expression assays

Gene	Assay ID
AFP	Hs01040607_m1
ALB	Hs00910225_m1
CYP3A4	Hs00430021_m1
CYP7A1	Hs00167982_m1
CYP2D6	Hs02576168_g1

17. Oncostatin M (OSM) (R&D Systems).
18. Dexamethasone (Sigma).
19. Type I collagen (Nitta Gelatin, Osaka, Japan).
20. Type I collagen-coated 12-well plate (15 μg/cm²): Dilute type I collagen in PBS for a final dilution of 1:50. Add 1 ml of type I collagen solution to coat each well of a 12-well plate. Incubate the plates for 3–24 h at 37°C. Remove type I collagen solution immediately before use.

2.4. Analysis

1. Human fetal (22–40 weeks old) liver total RNA (Clontech Laboratories, Mountain View, CA).
2. Human adult (51 years old) liver total RNA (Clontech Laboratories).
3. RNeasy Plus Mini kit (Qiagen, Hilden, Germany).
4. Superscript VILO cDNA synthesis kit (Invitrogen).
5. Taqman gene expression assays (Applied Biosystems, Foster City, CA): The primer sequences are described in Table 1.
6. ABI PRISM 7700 Sequence Detector (Applied Biosystems).
7. P450-GloTM CYP3A4 Assay Kit (Promega, Madison, WI).
8. Rifampicin (Sigma).
9. Dimethyl sulfoxide (Sigma).
10. Luminometer (Berthold, Tokyo, Japan).

3. Methods

3.1. Adenovirus Vector Construction

1. Ad vectors were constructed by an improved in vitro ligation according to the method of Mizuguchi and Kay. (13, 14). The human HEX cDNA was inserted into pHMEF5, which contains the human elongation factor-1α (EF-1α) promoter, resulting in pHMEF-HEX.

2. The pHMEF-HEX was digested with I-CeuI/PI-SceI and ligated into I-CeuI/PI-SceI-digested pAdHM41-K7, resulting in pAd-HEX.
3. Ad-HEX, which contains the EF-1α promoter and a stretch of lysine residues (K7) peptides in the C-terminal region of the fiber knob, was generated and purified.
4. The vector particle (VP) titer was determined by using a spectrophotometric method (15).

3.2. In Vitro Definitive Endoderm Differentiation

1. Prepare human iPS cells, which were maintained on MEF on a gelatin-coated 25 cm^2 flask in human iPS cell culture medium (see Note 1).
2. Before the initiation of cellular differentiation, change the medium of human iPS cells for the defined serum-free medium hESF9.
3. Incubate the cells in a humidified atmosphere of 10% CO_2 and 90% air at 37°C overnight (see Note 2).
4. For induction of definitive endoderm, remove the hESF9 medium, add 1.0 ml Accutase per 25-cm^2 flask, incubate for 3 min at 37°C, and remove the Accutase (see Note 3).
5. Add 10 ml of cold hESF9 medium, resuspend the human iPS cells into a single cell suspension by pipetting, and centrifuge at $267 \times g$ for 3 min at 4°C (see Note 4).
6. Aspirate the supernatant and resuspend the cells with 10 ml of cold differentiation medium A and centrifuge them at $267 \times g$ for 3 min at 4°C.
7. Repeat step 6.
8. Aspirate the supernatant, and replace the medium with warm fresh differentiation medium A supplemented with 10 ng/ml bFGF and 50 ng/ml Activin A.
9. Transfer to a laminin-coated 12-well plate in a humidified atmosphere of 10% CO_2 and 90% air at 37°C (2.5×10^5 cells/well). The final volume of medium should be 1.0 ml per well (see Note 5).
10. Change the differentiation medium A supplemented with 10 ng/ml bFGF and 50 ng/ml Activin A every day.

3.3. In Vitro Hepatoblast Differentiation

1. After 5 days of culture, remove the medium, add 200 µl trypsin–EDTA per well, incubate the cells for 3 min at 37°C, and remove the trypsin–EDTA (see Note 6).
2. Resuspend the cell populations in 10 ml of cold trypsin inhibitor A and centrifuge them at $267 \times g$ for 3 min at 4°C.
3. Aspirate the supernatant, resuspend the cells in 10 ml of cold differentiation medium B, and centrifuge at $267 \times g$ for 3 min at 4°C.

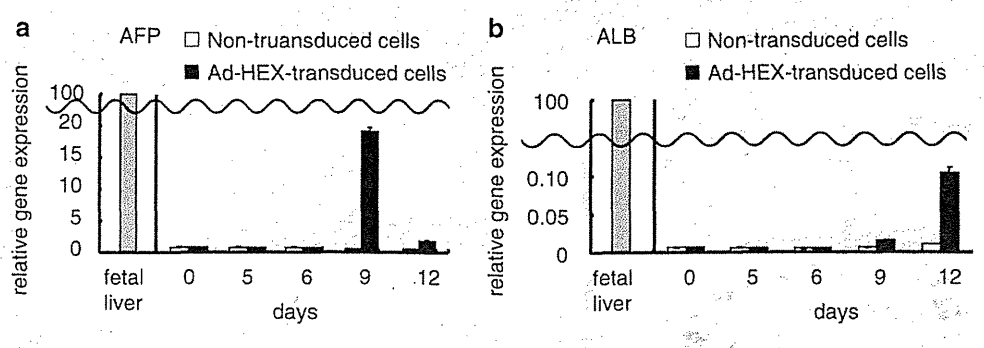

Fig. 2. Efficient hepatoblast differentiation from the human iPS cell-derived definitive endoderms by transduction of the HEX gene. Real-time RT-PCR analysis of the level of AFP (**a**) and ALB (**b**) expression in nontransduced cells and Ad-HEX-transduced cells, both of which were induced from the human iPS cell-derived definitive endoderms (day 0, 5, 6, 9, and 12). The cells were transduced with Ad-HEX at day 6 as described in Fig. 1. The data at day 6 were obtained before the transduction with Ad-HEX. The *graphs* represent the relative gene expression levels when the level in the fetal liver was taken as 100.

4. Aspirate the supernatant and replace with warm fresh differentiation medium B supplemented with 10 ng/ml bFGF and 50 ng/ml Activin A.
5. Transfer the cells to a laminin-coated tissue culture 12-well plate (5.0×10^5 cells/well) and culture them in a humidified atmosphere of 10% CO_2 and 90% air at 37°C. The final volume of medium should be 1.0 ml per well (see Note 5).
6. After 24 h of culture, remove the medium, and add warm fresh differentiation medium B supplemented with Ad-HEX (3,000 VP/cell), 10 ng/ml FGF4, and 10 ng/ml BMP4 (R&D Systems) (see Note 7). The final volume of medium should be 500 µl per well.
7. Incubate the cells in a humidified atmosphere of 10% CO_2 and 90% air at 37°C for 1.5 h.
8. Remove the medium and replace with warm fresh differentiation medium B supplemented with 10 ng/ml FGF4 and 10 ng/ml BMP4, and incubate the cells in a humidified atmosphere of 10% CO_2 and 90% air at 37°C.
9. Change the medium every day (see Note 8).
10. After 3 and 6 days of culture in differentiation medium B, analyze the cells by RT-PCR (see Note 9) (Fig. 2).

3.4. In Vitro Hepatic Maturation

1. After 3 days of culture in differentiation medium B, add 200 µl trypsin–EDTA in each well, incubate the cells for 3 min at 37°C, and remove the trypsin–EDTA.
2. Resuspend the cell populations in 10 ml of cold trypsin inhibitor B and centrifuge them at $267 \times g$ for 3 min at 4°C (see Note 10).